Available online at www.sciencedirect.com
SCIENCE DIRECT
Catalysis Today 114 (2006) 293–306
CATALYSIS TODAY
www.elsevier.com/locate/cattod

The influence of preparation method on the structure and redox properties of mesoporous Mn-MCM-41 materials

A. Derylo-Marczewska [a], W. Gac [b,*], N. Popivnyak [a], G. Zukocinski [a], S. Pasieczna [b]

[a] *Maria Curie-Skłodowska University, Faculty of Chemistry, Department of Adsorption, Maria Curie-Skłodowska Sq. 3, 20-031 Lublin, Poland*
[b] *Maria Curie-Skłodowska University, Faculty of Chemistry, Department of Chemical Technology, Maria Curie-Skłodowska Sq. 3, 20-031 Lublin, Poland*

Available online 3 April 2006

Abstract

Mesoporous silica materials modified by manganese have been prepared using surfactants containing different numbers of carbon atoms. Manganese has been introduced by the direct hydrothermal (HT), template ion-exchange (TIE) and impregnation methods. Structural properties have been investigated by the nitrogen adsorption–desorption, X-ray diffraction (XRD) and FT-IR studies. Redox properties have been investigated by the temperature-programmed reduction method (TPR) and transient CO oxidation reaction. It has been found that structural properties are strongly related to the type of surfactant used, the amounts and the way of Mn introduction. Large distortion effects are observed for samples prepared by the TIE method. Reducibility of the samples containing different pore dimensions and Mn loadings, prepared by TIE method, are very similar. Manganese oxide species in the catalysts of narrow pores and containing small amounts of manganese obtained by the HT and impregnation methods show low reducibility. During CO oxidation reaction some deactivation processes are observed for catalysts prepared by different methods and containing small amounts of Mn. A slight increase in activity for catalysts containing larger amounts of manganese is observed after high temperature treatment. Such changes are attributed to the interaction of manganese with silica and changes of oxidation state during thermal treatment.

Keywords: Manganese mesoporous silica materials; XRD; TPR; CO oxidation

1. Introduction

Since the discovery of the MCM-41 [1] and FSM-16 [2] in the early 1990s of the last century, great and fascinating progress has been made in the design, preparation, characterisation and application of mesoporous silica materials. Unique features of these materials are their regular structure, high surface area, extending 1000 m^2/g, and narrow pore size distribution in the range from 2 to 10 nm. Properties of these materials are easy to control using different preparation conditions, reagent ratios and thermal treatment conditions. In a typical synthesis of MCM-like materials silica skeleton is formed in a solution of suitable pH around self-assembled ionic or non-ionic surfactant micelles. Organic templates are removed by the calcination or extraction techniques [3,4]. It is well documented that pore diameter can be modelled using ionic surfactants with different numbers of carbon atoms in the hydrophobic alkyl chain [1,5], various oligomers or polymers as templates [6,7], suitable organic additives, such as 1,3,5-trimethylbenzene [8], as well as by the hydrothermal post-synthesis treatment [9,10].

Mesoporous silica materials have found wide application, e.g. in the adsorption processes and preparation of new nanostructured materials [11,12]. However, a real challenge is the application of these materials in the field of catalysis [13–17]. Attempts of improving the activity or thermal stability of pure silica materials have resulted in the preparation and successful application of a great number of new catalytic systems. The increase in thermal stability and changes of acid–base properties can be achieved by the incorporation of different ions, e.g. Al, Ti or Ga [18]. Modification of silica materials by addition of such ions as Cr, Fe, Co, V, Mo, Mn, Ru or Ce has yielded a new class of redox mesoporous catalysts [19–23]. In turn, the incorporation of small metal crystallites (e.g. Pt, Pd, Au, Ni or Cu) in the mesoporous silica materials has given interesting catalysts, utilised in the hydrogenation or oxidation reactions [24–27].

* Corresponding author. Tel.: +48 81 5375526; fax: +48 81 5375565.
E-mail address: wojtek@hermes.umcs.lublin.pl (W. Gac).

0920-5861/$ – see front matter
doi:10.1016/j.cattod.2006.02.066

A lot of attention has been paid to the preparation of hybrid inorganic–organic, very selective catalysts by introduction of various organic ligands. Different techniques have been developed for the preparation of modified silica mesoporous catalysts. In the direct hydrothermal method (HT), metal precursor is introduced directly into the synthesis mixture at the beginning of preparation process. In the template ion-exchange method (TIE), the metal ions are added into the as-synthesized silica material before template removal, and exchange the template cations. Finally the metal precursors can be introduced into the calcined silica materials (after complete removal of organic template) by simple impregnation techniques, chemical vapour deposition or more complex grafting methods.

The richness of the structures, oxygen mobility and often relatively low cost resulted in the wide applications and broad fundamental studies of the manganese catalysts [28,29]. Manganese is an active component of the redox catalytic systems, and can play either an oxidizing or reducing role ($Mn^{4+} \leftrightarrow Mn^{3+} \leftrightarrow Mn^{2+}$). The catalysts based on the bulk oxide systems, as well as supported catalysts, have been widely used in the deep and selective oxidation reactions of various organic compounds. These catalysts are utilised in the area of environmental chemistry, e.g. for abatement of volatile organic compounds or gaseous pollutants from combustion gases [30–32], and also in the field of organic synthesis, e.g. for selective oxidations of hydrocarbons or epoxidation of olefins [33,34]. Much attention has been focused on the preparation of complex catalytic systems containing manganese and noble metals such as Pd, Pt, Au or Ag [35–38].

After successful preparation of mesoporous pure silica materials several studies have been devoted to the introduction, characterisation and catalytic application of mesoporous manganese catalysts. Various techniques have been used for the preparation of such catalysts. In the DHT method manganese precursors such as chlorides [39,40], acetates [41–43] or nitrates [44] can be directly added to the synthesis mixture. Manganese has been also introduced by the TIE method developed by Iwamoto and co-workers [44–46]. Modification has also been performed using chemical vapour deposition method, e.g. by Caps and Tsang [47,48], or wet impregnation with different manganese salts [49]. A large number of papers have also been devoted to the incorporation of organic manganese complexes [50–56]. Mesoporous manganese catalysts have also been prepared using template assisted methods without silica, or using silica as the mesoporous template which is removed later by dissolution [57,58]. Such catalysts have been investigated in a broad range of catalytic oxidation processes, including epoxidation of styrene [44,51], olefins [53], oxidation of cyclohexane [41,55], ethylbenzene [42], styrene [56], sulfides [46], propene and CO [47], disproportionation of H_2O_2 [50]. In spite of extensive literature data, the influence of pore dimension on the redox properties of manganese oxide species in the mesoporous silica materials has not been widely studied. In the studies of Mn containing mesoporous silica catalysts the TPR technique is relatively rarely applied [48,59,60].

In the present paper, the structural and redox properties of the modified silica mesoporous materials containing different pore dimensions have been compared. Manganese has been introduced by three different ways. For characterisation of oxide species the TPR technique has been applied. This technique has been widely used in the studies of interactions between metal, oxygen and support in a large number of catalytic systems. As a simple catalytic test the CO oxidation reaction has been chosen. It is a well accepted opinion that the mechanism of carbon monoxide oxidation reaction is similar to that of hydrocarbon oxidation. It is often assumed that CO is chemisorbed on the surface of reducible oxide species, where it reacts with lattice oxygen, and then is desorbed as CO_2. The oxygen vacancy is filled up by adsorption of oxygen from the gas phase [47,61]. In our studies we have applied temperature-programmed technique with both temperature increase and decrease, which allowed us to observe some activation/deactivation processes.

2. Experimental

2.1. Catalyst preparation

Three series of materials characterised by different pore dimensions have been prepared. The silica MCM-41 materials have been synthesized using surfactant templates of different numbers of carbon atoms; dodecyltrimethylammonium bromide (MCM-41(12)), cetyl pyridinium chloride (MCM-41(16)), octadecyltrimethylammonium bromide (MCM-41(18)) and TEOS as silica source. In order to widen the pore diameters of MCM-41(18) materials 1,3,5-trimethylbenzene (TMB) was added to the reacting mixtures. The preparation procedure followed the method described in the literature [62]. In a typical synthesis of pure MCM-41 sorbent 6 g (MCM-41(12)), 7 g (MCM-41(16)) or 8 g (MCM-41(18)) of surfactant was dissolved in 360 cm^3 of distilled water. Ammonium hydroxide (25%) (30 cm^3) and weighed amount of TEOS (30 g) were added, and the mixture was stirred in thermostat for 1 h at 40 °C. The obtained product was filtered, washed with distilled water, dried at 80 °C for 2 h and calcined in air at 550 °C for 6 h.

The manganese ions were introduced to the catalyst by applying the direct hydrothermal synthesis, template ion-exchange [44,47] and wet impregnation techniques (Imp). In order to obtain materials with various metal contents different amounts of Mn precursor were added to the reacting mixtures. The obtained samples were coded A, B, C and D according to the increased loading. In the DHT method an aqueous solution of manganese(II) nitrate (1, 2 or 3 g of salt in 10 cm^3 of H_2O) as the metal ion precursor was added directly to the synthesis mixture before the hydrothermal process. Finally the product was filtered, washed, dried at 80 °C for 24 h and calcined in the same conditions as pure MCM-41 materials. In the TIE technique the template cations from the channels of the as-synthesized MCM-41 are exchanged with the metal ions in a solution. In the procedure to the as-synthesized MCM-41 sample an aqueous solution of manganese(II) nitrate was added

(1, 2 or 3 g of salt in 50 cm^3 of H_2O). The mixture was stirred vigorously at ambient temperature for 1 h, and then kept at 80 °C for 20 h. Finally the product was treated as in the case of previous materials.

The third group of samples has been obtained by impregnation of the original MCM-41(18) material with a solution of manganese salt. Samples of pure MCM-41(18) support were suspended in an aqueous solution of manganese(II) nitrate, stirred at ambient temperature, dried and calcined at 550 °C for 6 h. We have prepared several samples by this method: one containing small amount of manganese, and as the reference, three samples containing large amounts of manganese, much less studied in the past.

2.2. Catalyst characterisation

The amounts of manganese in the catalysts were determined by applying the X-ray fluorescence (ED-XRF Canberra 1510, USA).

In order to estimate the values of parameters characterising the mesoporous structure of synthesized materials the nitrogen adsorption/desorption isotherms at −196 °C were determined volumetrically using ASAP 2405N analyser (Micromeritics Corp., USA). Before the experiment samples were outgassed ($\sim 10^{-2}$ Pa) at 200 °C.

The adsorption data were used to evaluate the BET specific surface area, S_{BET} (from the linear BET plots), and the total pore volume, V_t (from the adsorption at the relative pressure $p/p_o = 0.98$) [63]. The primary mesopore volume, V_p, was obtained from the α_s plot method [64]. This method is based on the comparison of nitrogen isotherm for a studied porous solid with the standard isotherm for a reference non-porous adsorbent. This standard reduced isotherm α_s is defined as the ratio of adsorption value corresponding to a given relative pressure p/p_o and the adsorption value at the point $p/p_o = 0.4$ (p is the gas pressure, p_o is the saturation pressure, $p/p_o = 0.4$ is the starting point of isotherm hysteresis loop for nitrogen adsorption). The macroporous silica gel LiChrospher Si-1000 was used as a reference adsorbent [64]. The mesopore structure was characterised by the distribution function of mesopore volume calculated by applying the Barrett–Joyner–Halenda (BJH) method [64].

The structures of the studied samples were investigated by the X-ray diffraction (XRD) method with the modified diffractometer DRON 3 (Russia) using Cu Kα radiation.

The primary mesopore diameter (w_d) was calculated from the XRD (1 0 0) interplanar spacing d using the following equation [65]:

$$w_d = cd\left(\frac{\rho V_p}{1+\rho V_p}\right)^{1/2}$$

where c is a constant equal to 1.213 for cylindrical pores [65] and ρ is the pore wall density assumed to be equal to that of amorphous silica—2.2 g/cm^3.

The infrared spectra were recorded by means of Bio-Rad Excalibur FT-IR spectrometer, equipped with MCT detector, over the 4000–400 cm^{-1} range at the resolution of 4 cm^{-1}. A sample of a catalyst was mixed and ground in an agate mortar with spectroscopically pure dry potassium bromide to a fine powder and then pressed to form a disk less than 1 mm thick. Interferograms of 16 scans were averaged for each spectrum.

The redox properties of the samples were investigated by the temperature-programmed reduction (TPR) method. Studies were carried out in the TPR apparatus AMI-1 (Zeton Altamira). To remove adsorbed species (e.g. CO_2) samples before reduction were heated in the mixture of 5% O_2/He (Praxair) up to 500 °C with the rate 10 °C/min, then after 0.5 h were cooled down to room temperature. The reduction process was conducted in the mixture of 6% H_2/Ar ($Q = 30$ cm^3/min) (Praxair). The rate of temperature increase was 10 °C/min. The evolved water was removed in a cold trap maintained in the LN_2–methanol mixture at −98 °C, placed between reactor and thermal conductivity detector (TCD). Calibration of the TCD was performed by injection of precise amounts of Ar in the H_2/Ar flow.

The measurements of CO oxidation were conducted in the same TPR apparatus coupled with the mass spectrometer HAL201RC (Hiden Analytical). Samples ($m = 0.02$ g) were initially heated in the mixture of 5% O_2/He up to 500 °C, then were cooled down after 0.5 h. In the test reaction stage, samples were heated at the rate 10 °C/min up to 800 °C in the mixture of 0.5% CO, 2.5% O_2 and helium at the flow rate 40 cm^3/min, then were cooled down after 0.5 h. During experiments signals corresponding to CO ($m/e = 28$), oxygen ($m/e = 32$), CO_2 ($m/e = 44$) and H_2O ($m/e = 18$) were simultaneously collected.

3. Results and discussion

3.1. Structural properties of catalysts

The structural properties of the mesoporous silica materials have been extensively studied by many research groups. It was found that the internal space of MCM-41 silica materials is composed of regular, parallel pores with uniform dimensions. Their presence is identified by the distinct step on the nitrogen adsorption–desorption isotherms (IV type in the IUPAC classification) [63]. The arrangement of pores is usually studied by the XRD technique in the low-angle area. The MCM-41 structure is evidenced by the presence of four peaks, with a very strong peak at the low angle (1 0 0 reflection line), and three weaker peaks at the higher angle (1 1 0, 2 0 0 and 2 1 0 reflection lines) [14]. It was shown that the location of the main peak (1 0 0) moves to lower values with an increase in the alkyl chain length of the surfactant templates used for the preparation of MCM-41 materials [66].

The isotherms and pore size distributions for selected samples are shown in Figs. 1 and 2, respectively. The calculated values of the specific surface area, pore volume and dimension are included in Table 1. The course of isotherms for pure silica and for the materials modified by manganese indicates the presence of mesopores. In the case of pure silica materials, the value of p/p_o, at which sharp step is observed, gradually increases with an increase in the alkyl chain used for preparation, indicating the increase in pore dimension.

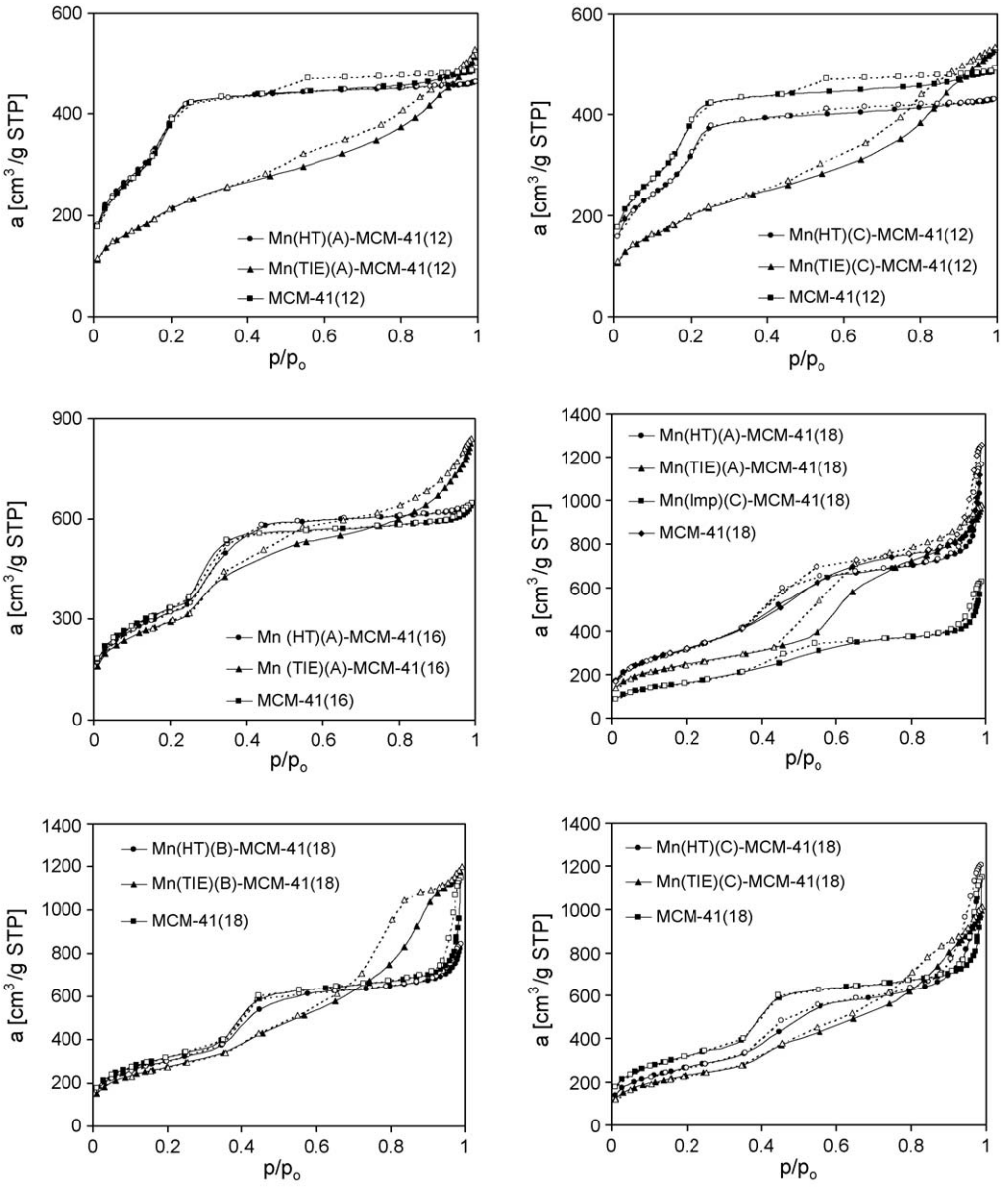

Fig. 1. Comparison of nitrogen adsorption/desorption isotherms for pure and selected Mn containing silicas.

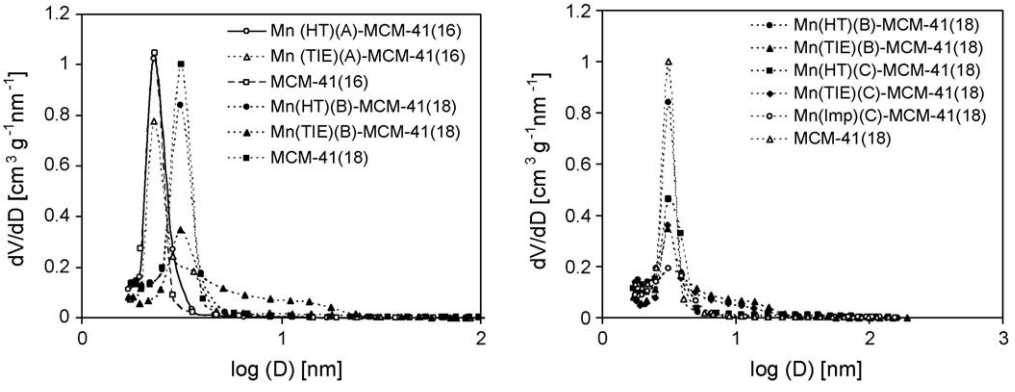

Fig. 2. Comparison of pore size distributions for selected pure and Mn containing silicas.

Table 1
Parameters characterising structure properties of synthesized MCM materials

Sample	Mn (wt.%)	S_{BET} (m^2/g)	V_t (cm^3/g)	V_p (cm^3/g)	d_{100} (nm)	w_d (nm)
MCM-41(12)	–	1320	0.75	0.63	3.18	2.94
Mn(TIE)(A)-MCM-41(12)	2.2	750	0.78	0.62	3.68	3.39
Mn(TIE)(C)-MCM-41(12)	4	700	0.81	0.75	3.74	3.58
Mn(HT)(A)-MCM-41(12)	2.2	1350	0.71	0.68	3.48	3.27
Mn(HT)(C)-MCM-41(12)	4.1	1110	0.66	0.64	3.62	3.36
MCM-41(16)	–	1190	0.97	0.82	4.07	3.96
Mn(TIE)(A)-MCM-41(16)	2.2	1050	1.24	0.82	4.23	4.12
Mn(HT)(A)-MCM-41(16)	2.2	1150	0.98	0.90	3.86	3.82
MCM-41(18)	–	1140	1.35	0.81	4.21	4.09
Mn(TIE)(A)-MCM-41(18)	2.4	880	1.45	0.67	6.22	5.82
Mn(TIE)(B)-MCM-41(18)	4.4	990	1.79	1.48	4.65	4.93
Mn(TIE)(C)-MCM-41(18)	4.2	820	1.49	0.96	4.55	4.55
Mn(HT)(A)-MCM-41(18)	1.9	815	1.3	0.41	4.75	4.50
Mn(HT)(B)-MCM-41(18)	4.5	1090	1.22	0.79	4.33	4.18
Mn(HT)(C)-MCM-41(18)	8.4	950	1.63	0.55	4.42	3.97
Mn(Imp)(A)-MCM-41(18)	3.7	1010	1.30	–	–	–
Mn(Imp)(B)-MCM-41(18)	18.3	490	0.54	–	–	–
Mn(Imp)(C)-MCM-41(18)	23.6	580	0.81	–	–	–
Mn(Imp)(D)-MCM-41(18)	34.2	45	0.15	–	–	–

The pore size distributions (PSD) calculated by BJH method evidence the uniformity of pore systems. The presence of well-resolved peaks on the XRD curves (Fig. 3), which can be attributed to the (1 0 0), (1 1 0) and (2 0 0) reflection lines, indicates a regular arrangement of pores in these materials. In accordance with literature data [66], we have observed a shift of the main peak on the XRD curves (1 0 0 reflection line) to lower angles.

The structural properties of the samples prepared by the introduction of small amounts of manganese nitrate into the synthesis mixture containing dodecyltrimethylammonium bromide or cetyl pyridinium chloride surfactants are similar to that of pure silica materials. The shape of nitrogen isotherms and the pore size distributions are very similar. However, a decrease in the intensity and smoothness of the peaks on the XRD curves may indicate a slight decrease in the uniformity of

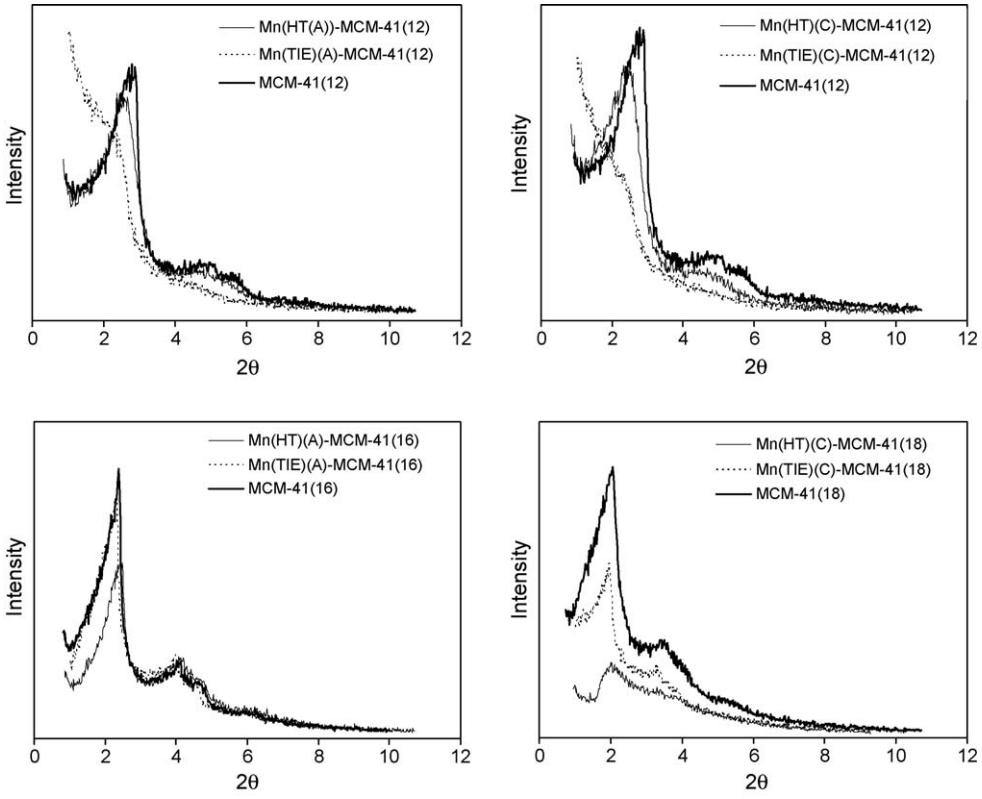

Fig. 3. XRD patterns for selected pure and Mn containing silica materials.

pore arrangement. When manganese content increases such effects become more visible. We can observe a decrease in the specific surface area and an increase in the pore volume. The pore size distributions are broader. Similar effects are observed for the samples prepared with surfactant of longer alkyl chain length. It should be noted that in the case of the Mn(HT)-MCM-41(18) samples pore dimension decreases with an increase in Mn contents. A different situation is observed for the catalysts prepared by the TIE method. The samples show much more visible changes of the structure. The isotherms for the Mn(TIE)-MCM-41(12) samples indicate a nearly amorphous nature of silica materials. We can observe large decrease in the specific surface area and an increase in the pore dimension. Similar, but not so strong effects are also visible for the Mn(TIE)-MCM-41(16) and Mn(TIE)-MCM-41(18) samples. Such results are rather surprising. We could expect more dramatic changes in the samples prepared by a direct introduction of manganese, where the presence of additional ions in the solution could disturb the processes of micelle organization and formation of the silica skeleton. Iwamoto and Tanaka [46] studied modified mesoporous silica materials obtained by the TIE method. In the series of catalysts containing up to 2.9 wt.% Mn they observed a little collapse of the structure, but no change in the hexagonal array of mesopores. On the contrary Dong et al. [67] observed a gradual increase in the distortion effects with an increase of manganese contents in the Mn-loaded mesoporous silica MCM-41 prepared via reducing $KMnO_4$ with in situ surfactant, especially for Mn-rich samples. In turn, Zhang et al. [44] noticed a serious decrease in regularity for a series of Mn-MCM-41 catalysts synthesized by the HT method containing up to 1.9 wt.% Mn. In the samples prepared by the TIE method (even for that containing around 1.5 wt.% Mn) they did not observe a significant deorganization of the mesoporous structure. Similar changes were also observed by Wang et al. [39] for the samples obtained by a direct introduction of $MnCl_2$ into the synthesis mixture. They suggested that the distortion of the structure of MCM-41 materials may result from partial substitution of Mn for Si, leading to a looser structure of the walls, a stronger contraction effect during calcinations or a lower condensation degree of silicate oligomers. Wang also pointed out the possibility of the formation of $Mn(OH)_2$ species, their non-uniform distribution, and as a result, the coexistence of hexagonal and lamellar structures in some area. It was found that mesoporous manganese oxides can be prepared using similar procedures as in the case of pure silica materials. For example, Sun et al. [68] showed that in a solution of the proper ratio of OH^-/Mn^{2+}, the OH^- or $[Mn(OH)_6]^{4-}$ ions are located around self-assembled cetyltrimethylammoniom cations and the Mn^{2+} cations form layered manganese oxide mesophases. These examples indicate that the complex processes occur in the systems containing manganese salts, surfactant molecules and silica. In the light of the above presented studies the nature of the distortion effects in the manganese samples obtained by TIE method is not quite clear. One of the reasons could be the rate of the exchange process, which can be related to temperature, cations concentration and the size of surfactant molecules. However, further studies are needed to confirm this hypothesis.

We have also studied modified mesoporous silica materials obtained by the impregnation technique. Fig. 1 shows the isotherms for selected samples. The structural properties of the low loaded catalysts are similar to the samples prepared by HT technique. However, the introduction of large amounts of manganese causes the smoothing of the isotherms. The specific surface area decreases to low values; S_{BET} for the samples containing 34 wt.% Mn equals 45 m^2/g. The reason for such changes is slightly different to that discussed above. After removal of the template molecules by calcinations, silica material is rather stable. Although during impregnation some processes of silica reconstruction or dissolution may occur after immersion of the sample in a solution, however, a more probable explanation is the presence of large manganese oxide species, which are confined in the channels of the MCM-41 material.

3.2. XRD studies

The XRD patterns in the high angle area for the samples obtained by the HT, TIE techniques, and even by impregnation with small amounts of manganese, show no distinct reflection of manganese oxide phases (Fig. 4). This suggests the presence of very small, well dispersed species within the silica matrix or on the silica walls.

All materials exhibit a broad silica peak around 23° indicating a low overall degree of crystallization of siliceous walls. The XRD curves for the samples synthesized by the hydrothermal method reveal only slight diffraction peaks, which cannot be attributed to one type of manganese oxide. They indicate the coexistence of different manganese oxides of low crystallinity, which do not form a distinct crystalline structure. However, the XRD curves for the samples containing 20–30 wt.% of Mn show distinct diffraction peaks. For Mn(Imp)(C)-MCM-41(18) sample peaks located at the values of 2θ equal to 29°, 38°, 41°, 43°, 57° and 59° indicate the formation of tetragonal $P42/mnm$ MnO_2 species (JCPDS Card 81-2261).

3.3. FT-IR spectroscopy

Fig. 5 shows the framework vibration FT-IR spectra for the selected samples containing manganese and pure silica materials with different pore dimensions. The absorption bands at around 1030 and 1080 cm^{-1} are due to asymmetric stretching vibrations of Si–O–Si bridges. The absorption band at 960–970 cm^{-1} is connected with the stretching vibrations of the Si–OH groups, while the bands at 780–800 and 540–560 cm^{-1} are the symmetric stretching vibrations of Si–O–Si bridges. The bands located at 450–460 cm^{-1} are assigned to the Si–O bending vibration [69,70]. In the samples obtained by the TIE method one can observe broadening of the peaks located between 1000 and 1300 cm^{-1}, which can be attributed to more amorphous nature of these materials. The increase in band intensity located at 960–970 cm^{-1} is often assigned to the presence of stretching vibration of the Si–O–Me linkage.

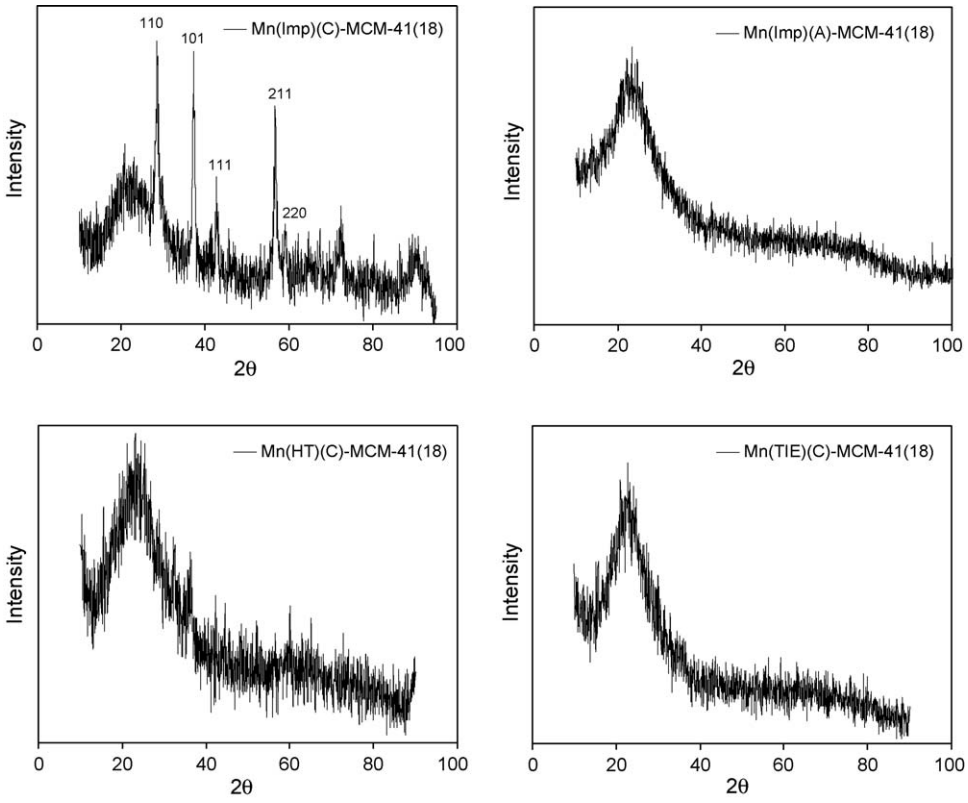

Fig. 4. XRD patterns for selected samples.

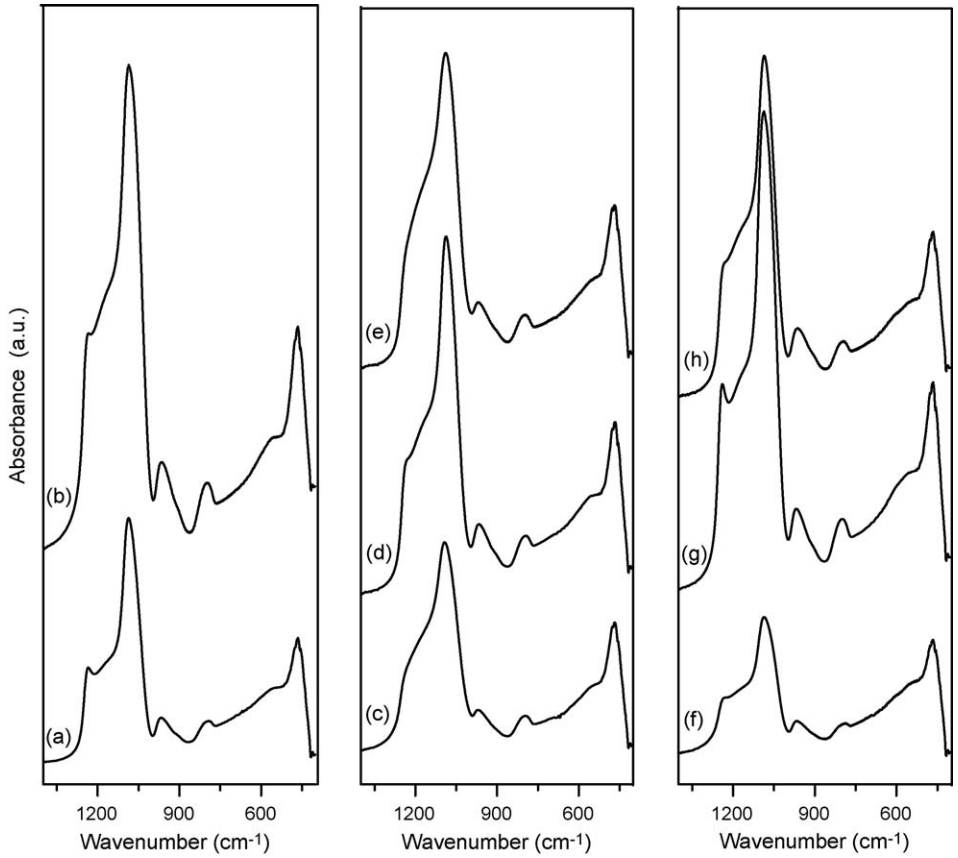

Fig. 5. FT-IR spectra for selected samples: (a) MCM-41(12), (b) MCM-41(18), (c) Mn(TIE)(C)-MCM-41(12), (d) Mn(TIE)(A)-MCM-41(16), (e) Mn(TIE)(B)-MCM-41(18), (f) Mn(HT)(C)-MCM-41(12), (g) Mn(HT)(A)-MCM-41(16) and (h) Mn(HT)(B)-MCM-41(18).

This effect and a slight decrease in frequencies indicate the incorporation of metal into the framework [39,71–74]. The intensity of the band at 960–970 cm^{-1} is lower for the samples obtained by the TIE method than for the Mn(HT) samples. Such an effect noted for the samples of different pore dimensions may result from partial incorporation of Mn into the silica framework.

3.4. Temperature-programmed reduction studies

The differences between manganese catalysts are well evidenced by the TPR curves (Fig. 6; Table 2). The shape of the reduction curves for the samples prepared by the TIE method is very similar and is not related to pore diameter of silica support. One can observe a broad peak located in the range 200–500 °C.

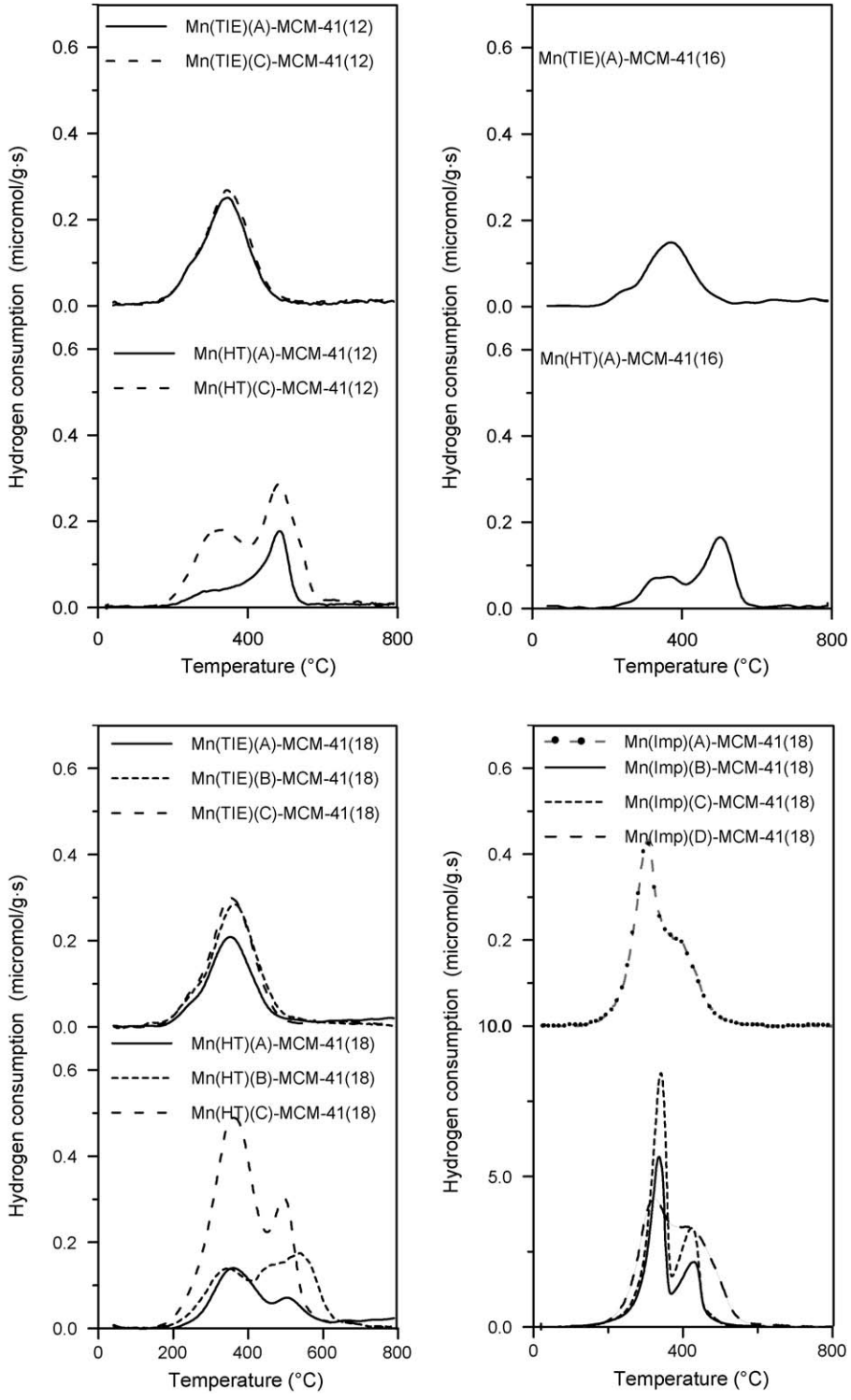

Fig. 6. TPR curves of the catalysts.

Table 2
Hydrogen consumption, average oxidation number of Mn calculated from the TPR measurements and temperatures of 25, 50 and 75% CO conversion

Sample	Hydrogen consumption (mmol/$g_{cat.}$)	Average oxidation number of Mn	Temperatures of CO conversion (°C)		
			25%	50%	75%
Mn(TIE)(A)-MCM-41(12)	0.243	3.19	405	495	722
Mn(TIE)(C)-MCM-41(12)	0.260	2.71	405	500	750
Mn(HT)(A)-MCM-41(12)	0.132	2.66	561	778	–
Mn(HT)(C)-MCM-41(12)	0.345	2.93	423	523	–
Mn(TIE)(A)-MCM-41(16)	0.175	2.89	382	571	744
Mn(HT)(A)-MCM-41(16)	0.158	2.79	347	384	743
Mn(TIE)(A)-MCM-41(18)	0.232	3.05	458	607	772
Mn(TIE)(B)-MCM-41(18)	0.302	2.76	479	607	697
Mn(TIE)(C)-MCM-41(18)	0.313	2.78	451	579	697
Mn(HT)(A)-MCM-41(18)	0.246	3.39	605	742	797
Mn(HT)(B)-MCM-41(18)	0.289	2.71	521	661	771
Mn(HT)(C)-MCM-41(18)	0.495	2.64	429	535	697
Mn(Imp)(A)-MCM-41(18)	0.298	2.88	430	590	–
Mn(Imp)(B)-MCM-41(18)	2.628	3.58	200	249	–
Mn(Imp)(C)-MCM-41(18)	3.853	3.80	260	298	321
Mn(Imp)(D)-MCM-41(18)	4.497	3.44	224	274	316

The shape of the peak indicates two noticeable overlapping reduction processes. The oxide species in the samples prepared by the HT method are more difficult to reduce. The curves show two distinct peaks located in the range 200–450 and 450–650 °C. In the case of the samples containing smaller pores higher hydrogen consumption is observed in the second region. The opposite tendency is visible in the samples containing large pores. Similar and even more resolved peaks occur on the curves of the impregnated samples. However, their location is similar to the peaks of the samples prepared by TIE method.

The reduction of bulk manganese oxides is often described by the following sequential process: $MnO_2 \rightarrow Mn_2O_3 \rightarrow Mn_3O_4 \rightarrow MnO$. The direct assignment of peaks on the TPR curves to the consumption of hydrogen in the above described process is very difficult. Manganese oxides often occur as non-stoichiometric systems, and easily change their bulk or surface properties. The composition and structure of manganese oxides is strongly related to the preparation method and thermal treatment conditions. According to the literature data decomposition of the manganese nitrate to MnO_2 occurs at the temperatures 200–300 °C [75]. MnO_2 heated in air at 500–600 °C gives Mn_2O_3. In more severe conditions (940–960 °C and above 1160 °C) Mn_2O_3 is transformed into Mn_3O_4 and MnO, respectively [29,76,77]. Formation of the Mn_2O_3 or Mn_3O_4 is usually enhanced, when carbonates or salts containing carbon molecules are used. In the case of supported systems the nature of the manganese oxide species is influenced by the MnO_x–support interaction [78–80]. It has been reported that in the catalysts containing small amounts of manganese the dominating role of support is stabilization of the low-valence manganese oxide species [81]. Often at low manganese loading the isolated Mn^{2+}, Mn^{3+} or even Mn^{4+} species coexist on the surface. At increased loading the amounts of Mn^{3+} or Mn^{4+} species increase and two-dimensional layered or amorphous structures are formed [81,82]. In the Mn-rich systems the support enhances dispersion of the large three-dimensional species, which results in an increase in reducibility.

The results of hydrogen consumption in the TPR measurements of the impregnated Mn-rich samples Mn(Imp)(B)MCM-41(18) indicate the presence of MnO_2 species. The first peak on the TPR curve can be ascribed to the reduction of MnO_2 to Mn_3O_4, and the second to the reduction of Mn_3O_4 to MnO. As Mn loading increases, the average oxidation number of Mn slightly decreases. The observed phenomena may result from worse stability of those oxide species, well resembling bulk oxide phases [58]. The obtained results are in good correlation with XRD data. A similar shape of the TPR curve for Mn(HT)(A)-MCM-41(18) sample may indicate the presence of similar species. However, due to lack of visible XRD patterns, and lower oxidation number of Mn, the oxide species appear to be much smaller, well dispersed on the silica surface, and mostly in the form Mn^{3+} or Mn^{2+}.

The broadening of the TPR peaks observed in the samples prepared by hydrothermal method can be ascribed to the presence of species with different reducibilities, resulted from a different strength of Mn–O interactions. A shift of maximum reduction peak towards higher temperatures, which is usually regarded as the indication of strong interaction between oxide species and support, evidences the presence of MnO_x species strongly bounded to silica walls or incorporated in the silica framework. As Mn loading increases the stabilizing role of support is less visible, and probably larger species are formed. The shape of the TPR curves becomes more similar to the reduction curves of bulk MnO_2 phases. However, considering the changes of the oxidation number we can suppose that still a large number of Mn^{2+} cations are bounded to the surface or incorporated into the silica framework. Similar changes are observed for the catalysts based on the MCM-41(12) materials with smaller pores. However, these catalysts contain manganese oxide species of lower oxidation number, more strongly interacting with silica support. An increase in manganese loading causes an increase in the number of Mn^{3+} or even Mn^{4+} ions. A similar dependence of pore dimension on reducibility was reported by Khodakov et al. for cobalt impregnated

supported mesoporous silicas [60]. They observed the formation of small Co_3O_4 particles in narrow pore supports, which were more difficult to reduce than larger species in wider pores. They ascribed such differences to a much stronger interaction between smaller metal oxide species and support. The spectroscopic studies of the Mn-MCM materials containing small amounts of Mn and prepared by a similar HT method pointed to the coexistence of Mn^{2+} and Mn^{3+} ions coordinated with Si(IV) by disordered octahedral or tetrahedral environments [40,43,83,84] and partial substitution of Si^{4+} in the framework position by Mn^{3+} [44]. Using ESR and ^{20}Si MAS NMR technique Yuan et al. [85] evidenced the presence of framework of manganese ions in the as-synthesized or calcined forms. They found the oxidation of framework of Mn^{2+} to Mn^{3+} during calcinations, and the reduction of Mn^{3+} to Mn^{2+} by H_2 at elevated temperatures. They also observed the migration of the extraframework of Mn^{2+} in hydrogen atmosphere to the manganese cations in framework positions. A similar coexistence of different manganese cations was observed by the XANES and EXAFS techniques. It was shown [86] that during calcination complex processes occur which involve the changes of the valence state of most manganese cations from Mn^{2+} to Mn^{3+} and the rearrangement of the Mn^{2+} cations in the extraframework positions to framework position.

The coexistence of different MnO_x species was also reported for Mn containing MCM materials prepared by the TIE method. It was shown that Mn^{2+} or Mn^{3+} ions are located mainly on the surface of silica support [44–46]. We stated different shapes of the TPR curves for Mn(TIE) and Mn(HT) samples. A more uniform shape of the TPR is probably related to the presence of the species with similar reducibility, regardless of Mn loading and pore dimension. It is very intriguing that the amount of hydrogen consumed during reduction is not a straight function of the Mn loading. Such effects may result from the existence of manganese species in the form of Mn^{2+} ions, which cannot be reduced in the TPR conditions. An increase in Mn loading causes an increase in the number of Mn^{2+} cations located on the silica surface. In these samples, in contrast to the samples obtained by the hydrothermal method, the effect of pore dimension is not strongly manifested. Moreover, in spite of the more or less perfect porous structure, samples prepared by TIE technique with different templates show similar reducibility, which indicates the similar nature of the manganese species. It means that during catalytic reactions, the overall rate or selectivity can be related to the total number of manganese surface species and also, especially for large molecules, can be controlled by the diffusion effects related to the pore dimension.

3.5. CO oxidation reaction

Fig. 7 shows the effects of pore dimension, preparation method and Mn loading on the catalytic activity of catalysts in the oxidation of CO. The measurements were conducted in a temperature-programmed manner, using temperature increase and then decrease, with the maximum at 800 °C. The activity of catalysts was compared on the basis of temperatures which correspond to a given conversion degree T_{25}, T_{50} and T_{75} (during temperature increase) (Table 2).

The catalysts obtained by the TIE, HT and impregnation methods, which contain small amounts of manganese, show relatively low activity in the CO oxidation reaction. For most samples the temperature T_{25} is above 400 °C. The changes of activity are related to the pore dimension, the way of Mn introduction and Mn loading. In the case of samples prepared by the TIE method the initial activity of Mn(TIE)-MCM-41(12) samples is higher than for Mn(TIE)-MCM-41(18) catalysts. The temperatures of 50% CO conversion increase with increasing pore dimension (the catalysts show lower activity). However, after high temperature treatment (at 800 °C for 0.5 h), the activity of the Mn(TIE)-MCM-41(12) catalysts decreases, for Mn(TIE)-MCM-41(16) is comparable and for Mn(TIE)-MCM-41(18) becomes even better. This effect is also partially associated with Mn loading. In the case of samples with smaller pores, the effect of Mn loading is practically not observed. For the samples containing larger pores the initial activity is very similar, but after reaction performed at 800 °C increases with increasing manganese content. The increase in activity was not a straight function of reaction temperature. In some ranges of reaction temperature activity increased more slowly or even decreased. Such behavior can be explained by the changes of the oxidation number of manganese and migration of manganese on the surface of silica or between framework and extraframework positions. As we have mentioned above, in the samples prepared by the TIE method most of the Mn ions are located on the silica surface. Probably, during reaction at high temperature some of the Mn^{2+} ions are oxidized to Mn^{3+} which leads to an increase in activity. Simultaneously Mn^{2+} and/or Mn^{3+} can be incorporated into the silica framework which causes a decrease in activity. High activity of manganese catalysts is often regarded as a result of the presence of labile oxidation state of Mn, usually due to the presence of Mn^{3+} or Mn^{4+} ions [48,61,87,88]. Thus, an incorporation of Mn ions into the silica framework during high temperature treatment, particularly in the systems of smaller pores or containing small amounts of Mn, decreases such an ability.

Samples prepared by the hydrothermal method show slightly different changes of activity. In the series containing ~2 wt.% Mn, just like the catalysts prepared by TIE method, the catalysts based on the octadecyltrimethylammonium bromide surfactant (MCM-41(18)) show lower activity. This effect could be related to the lower dispersion of Mn oxide species confined in the large pores [60,89]. However, the activity of Mn(HT)MCM-41 catalysts strongly increases with an increase in Mn loading. It should be noted that low temperature peaks on the TPR curves increase similarly. The activation/deactivation processes are also visible, and similar trends are observed. The catalysts containing smaller pores or smaller amounts of manganese deactivate more easily at high temperature. The activity of catalysts prepared by the hydrothermal method can be controlled by pore dimension, Mn loading and high temperature treatment. Fig. 8 shows changes of activity (the temperature of 25% CO conversion) for catalysts containing different pore dimensions prepared by

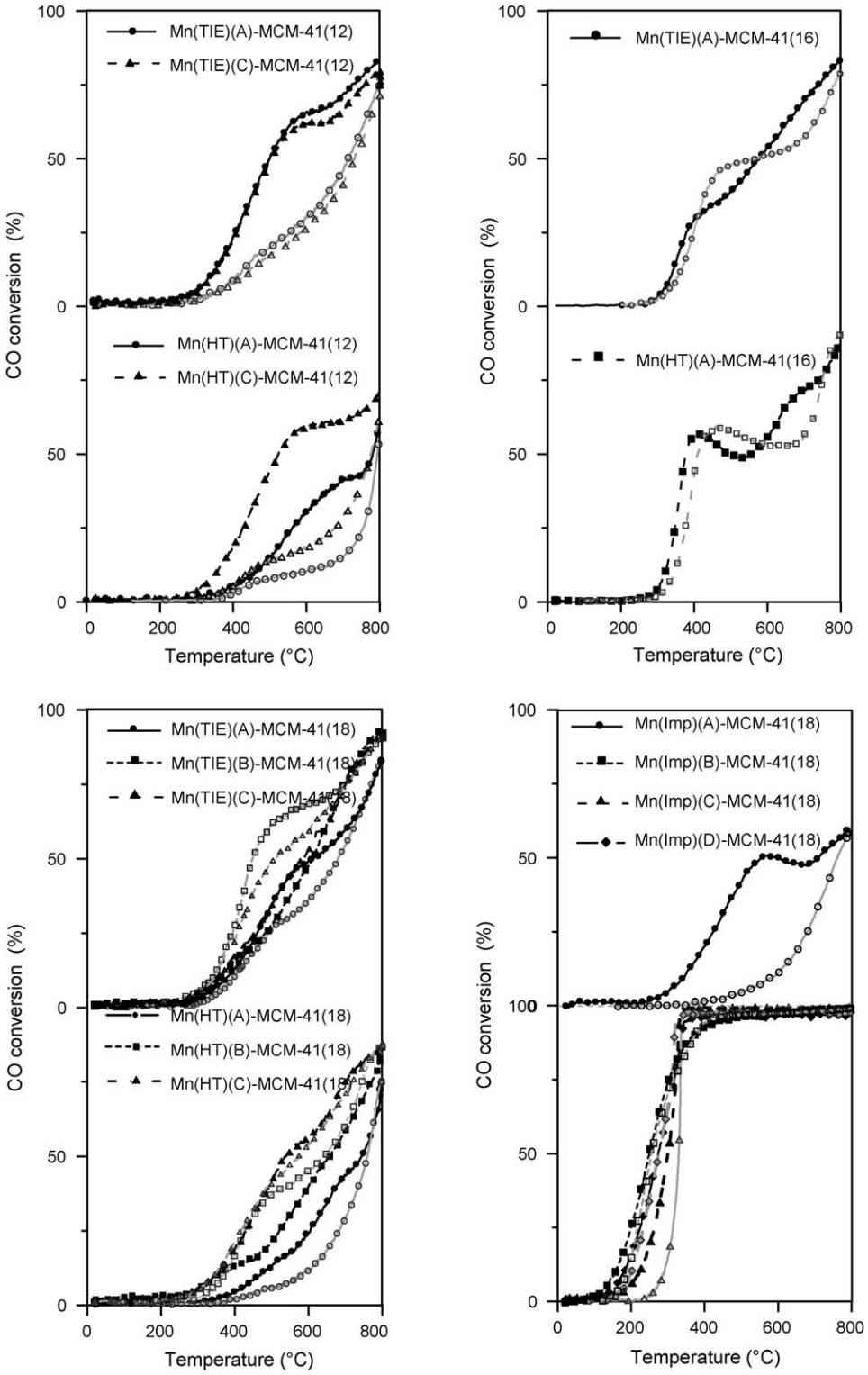

Fig. 7. Temperature-programmed reaction oxidation of CO. Dark lines with filled symbols—temperature increase; grey lines with open symbols—temperature decrease.

the hydrothermal and template ion-exchange methods. It seems that for the samples prepared by HT method there is an optimal range of pore dimension which corresponds to higher activity. For the catalysts prepared by TIE such a relationship is less visible.

Much higher activity is observed for Mn-rich catalysts prepared by the impregnation method (Fig. 8b). For the Mn(Imp)(D)-MCM-41(18) sample the initial temperature of CO oxidation is about 100 °C. With an increase of reaction temperature a sigmoidal increase is observed. CO conversion

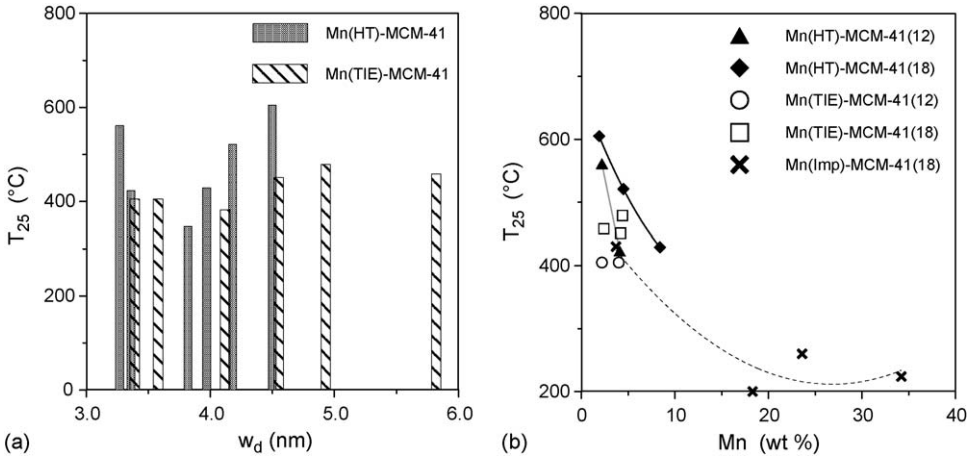

Fig. 8. The temperatures of 25% CO conversion in the samples of different pore widths (a) and Mn loadings (b).

approaches high values (90–100%) at temperature 350–400 °C. Similar activity is still observed after high temperature treatment in reaction conditions at 800 °C for 0.5 h. The decreasing lines reveal very slight deactivation phenomena, which can be attributed to a partial decomposition of the MnO_x phases. When Mn loading decreases to 18% only a small decrease of activity is observed. In the case of impregnated catalysts containing small amounts of Mn we observe much lower activity, comparable to the catalysts prepared by the HT method. Similar deactivation effects are visible. These findings confirm previous results of the oxidation reactions of various compounds over manganese catalysts [61,87,88]. The presence of strong interaction in smaller pores may be responsible for the formation of smaller oxide species, as well as enhanced incorporation of manganese to the silica walls. An increase in activity of manganese catalysts has often been improved by special preparation techniques and changes in composition, which resulted in an increase in oxygen mobility or increase in manganese oxide dispersion. High activity of the Mn-MCM-41 in the CO oxidation reaction was observed by Gleeson et al. [47] for the catalysts prepared by chemical vapour deposition with $Mn_2(CO)_{10}$. They ascribed high activity to the presence of well dispersed manganese species on the silica wall. Enhanced reducibility of such species in the catalysts was evidenced by Caps and Tsang [48]. The influence of pore size on the activity of catalysts was often associated with different amounts of ligands which could be attached to the pore surface. Choi et al. [59] observed that the amount of functionalized species increased with the pore diameters of MCM-41 to a threshold pore size.

We have shown that the activity of the studied catalysts in the CO oxidation reaction was not very high, especially when we compare some bulk manganese oxides [35,92] or gold supported manganese catalysts [90,91], which can oxidize CO below room temperature. However, silica mesoporous manganese catalysts bear interesting structural and redox properties, controlled by the pore dimension, the way of manganese introduction and loading, which can be attractive for more demanding catalytic processes due to high surface area, pore uniformity as well as for preparation of new complex catalytic systems.

4. Conclusions

We have shown that structural and redox properties of Mn-MCM-41 catalysts can be adjusted by the proper choice of the preparation method, surfactant template and Mn loading. We have prepared a series of modified silica mesoporous catalysts with varied pore dimension using different procedures of Mn introduction. Pore dimension was controlled by applying surfactants of different alkyl chain lengths. An introduction of manganese by the template ion-exchange method caused strong distortion effects of the ordered silica structure, less evidenced in the samples containing larger pores. An increase in manganese loading caused slight changes of reducibility and activity in the CO oxidation reaction. High reaction temperature caused some activation/deactivation processes, resulting from the changes of Mn oxidation state and interaction with silica framework. Samples of similar Mn loading containing larger pores showed lower activity. An increase in manganese loading in the samples prepared by the hydrothermal and impregnation methods enhanced reducibility and activity. The TPR results indicated the coexistence of different manganese species. In the samples of different pore dimensions and manganese loadings prepared by the TIE method, the nature of the species, identified as well dispersed, strongly interacting with silica surface was similar. In the case of samples prepared by the hydrothermal method the effect of pore dimension was more complex. Narrow pores of silica materials caused the formation of small species strongly interacting with silica surface or incorporated into the framework. An increase in Mn loading and pore diameter favoured formation of larger particles weakly interacting with silica support. We have observed that the presence of small oxide species of the size partially controlled by pore dimension or preparation method, and simultaneously not strongly interacting with silica support can increase activity in the CO oxidation reaction.

Acknowledgement

This work was supported by the Polish Ministry of Education and Science as research project 3T09B11429.

References

[1] J.S. Beck, J.C. Vartuli, W.J. Roth, M.E. Leonowicz, C.T. Kresge, K.D. Schmitt, C.T.-W. Chu, D.H. Olson, E.W. Sheppard, S.B. McCullen, J.B. Higgins, J.L. Schlenker, J. Am. Chem. Soc. 114 (1992) 10834.
[2] T. Yanagisawa, T. Shimizu, K. Kuroda, C. Kato, Bull. Chem. Soc. Jpn. 63 (1990) 988.
[3] F. Kleitz, W. Schmidt, F. Schüth, Microporous Mesoporous Mater. 65 (2003) 1.
[4] D. Kumar, K. Schumacher, C. du Fresne von Hohenesche, M. Grün, K.K. Unger, Colloids Surf. A 187–188 (2001) 109.
[5] M. Kruk, M. Jaroniec, A. Sayari, Microporous Mesoporous Mater. 35–36 (2000) 545.
[6] D. Zhao, Q. Huo, J. Feng, B.F. Chmelka, G.D. Stucky, J. Am. Chem. Soc. 120 (1998) 6024.
[7] Y. Wang, M. Noguchi, Y. Takahashi, Y. Ohtsuka, Catal. Today 68 (2001) 3.
[8] S.K. Jana, R. Nishida, K. Shindo, T. Kugita, S. Namba, Microporous Mesoporous Mater. 68 (2004) 133.
[9] D. Khushalani, A. Superman, G.A. Ozin, K. Tanaka, J. Garces, M.M. Olken, N. Coombs, Adv. Mater. 7 (1995) 842.
[10] A. Sayari, P. Liu, M. Kruk, M. Jaroniec, Chem. Mater. 9 (1997) 2499.
[11] D. Zhao, P. Yang, Q. Huo, B.F. Chmelka, G.D. Stucky, Curr. Opin. Solid State Mater. Sci. 3 (1998) 111.
[12] F. Fajula, A. Galarneau, F. Di Renzo, Microporous Mesoporous Mater. 82 (2005) 227.
[13] X.S. Zhao, G.Q. Lu, G.J. Millar, Ind. Eng. Chem. Res. 35 (1996) 2075.
[14] S. Biz, M.L. Occelli, Catal. Rev. Sci. Eng. 40 (1998) 329.
[15] D.T. On, D. Desplantier-Giscard, C. Danumah, S. Kaliaguine, Appl. Catal. A 222 (2001) 299.
[16] D. Brunel, A.C. Blanc, A. Galarneau, F. Fajula, Catal. Today 73 (2002) 139.
[17] A. Taguchi, F. Schüth, Microporous Mesoporous Mater. 77 (2005) 1.
[18] A. Tuel, Microporous Mesoporous Mater. 27 (1999) 151.
[19] D.S. Lee, T.K. Liu, J. Sol–Gel Sci. Technol. 24 (2002) 69.
[20] R. Köhn, M. Fröba, Catal. Lett. 68 (2001) 227.
[21] V. Parvulescu, B.-L. Su, Catal. Today 68 (2001) 315.
[22] D. Wei, W.T. Chueh, G.L. Haller, Catal. Today 51 (1999) 501.
[23] S. Kawi, S.Y. Liu, S.-C. Shen, Catal. Today 68 (2001) 237.
[24] B.S. Uphade, Y. Yamada, T. Akita, T. Nakamura, M. Haruta, Appl. Catal. A 215 (2001) 137.
[25] J. Blanhard, K. Fajerwerg, M. Breysse, P. Beaunier, M.F. Ribeiro, J.M. Silva, P. Massiani, Catal. Lett. 3–4 (2002) 221.
[26] J. Okamura, S. Nishiyama, S. Tsuruya, M. Masai, J. Mol. Catal. A 135 (1998) 133.
[27] Y.S. Cho, J.C. Park, B. Lee, Y. Kim, J. Yi, Catal. Lett. 81 (2002) 89.
[28] Q. Feng, H. Kanoh, K. Ooi, J. Mater. Chem. 9 (1999) 319.
[29] F. Arena, T. Torre, C. Traimondo, A. Parmaliana, Phys. Chem. Chem. Phys. 3 (2001) 1911.
[30] M. Baldi, E. Finocchio, F. Milella, G. Busca, Appl. Catal. B 16 (1998) 43.
[31] J.I. Gutiérrez-Ortiz, R. López-Fonseca, U. Aurrekoetxea, J.R. González-Velasco, J. Catal. 218 (2003) 148.
[32] P. Fabrizioli, T. Bürgi, A. Baiker, J. Catal. 207 (2002) 88.
[33] T.M. Nenoff, M.C. Showalter, K.A. Saltz, J. Mol. Catal. A 121 (1997) 123.
[34] R. Krishnan, S. Vancheesan, J. Mol. Catal. A 185 (2002) 87.
[35] G.B. Hoflund, S.D. Gardner, D.R. Schryer, B.T. Upuchurch, E.J. Kielin, Appl. Catal. B 6 (1995) 117.
[36] M.C. Álvarez-Galván, B. Pawelec, V.A. de la Peña O'Shea, J.L.G. Fierro, P.L. Arias, Appl. Catal. B 51 (2004) 83.
[37] M. Ferrandon, J. Carnö, S. Järås, E. Björnbom, Appl. Catal. A 180 (1999) 153.
[38] N. Watanabe, H. Yamashita, H. Miyadera, S. Tominga, Appl. Catal. B 8 (1996) 405.
[39] L.Z. Wang, J.L. Shi, J. Yu, D.S. Yan, Nanostruct. Mater. 10 (1998) 1289.
[40] J. Xu, Z. Luan, T. Wasowicz, L. Kevan, Microporous Mesoporous Mater. 22 (1998) 179.
[41] W.A. Carvalho, P.B. Varaldo, M. Wallau, U. Schuchardt, Zeolites 18 (1997) 408.
[42] S. Vetrivel, A. Pandurangan, Appl. Catal. A 264 (2004) 243.
[43] S.Y. Yuan, H.T. Ma, Q. Luo, W. Zhou, Mater. Chem. Phys. 77 (2002) 299.
[44] Q. Zhang, Y. Wang, S. Itsuki, T. Shishido, K. Takehira, J. Mol. Catal. A 188 (2002) 189.
[45] M. Yonemitsu, Y. Tanaka, M. Iwamoto, Chem. Mater. 9 (1997) 2679.
[46] M. Iwamoto, Y. Tanaka, Catal. Surv. Jpn. 5 (2001) 25.
[47] D. Gleeson, R. Burch, N.A. Cruise, S.C. Tsang, Nanostruct. Mater. 12 (1999) 1007.
[48] V. Caps, S.C. Tsang, Catal. Today 61 (2000) 19.
[49] S. Vetrivel, A. Pandurangan, J. Mol. Catal. A 227 (2005) 269.
[50] J. Gao, A.E. Martell, Inorg. Chim. Acta 343 (2003) 343.
[51] G.J. Kim, S.H. Kim, Catal. Lett. 57 (1999) 139.
[52] D.W. Park, S.D. Choi, S.J. Choi, C.Y. Lee, G.J. Kim, Catal. Lett. 78 (2002) 145.
[53] S. Xiang, Y. Zhang, Q. Xin, C. Li, Chem. Commun. (2002) 2697.
[54] S. Gago, Y. Zhang, A.M. Santos, K. Köhler, F.E. Kühn, J.A. Fernandes, M. Pillinger, A.A. Valente, T.M. Santos, P.J.A. Ribeiro-Claro, I.S. Goncalves, Microporous Mesoporous Mater. 76 (2004) 131.
[55] S.H. Lau, V. Caps, K.W. Yeung, K.Y. Wong, S.C. Tsang, Microporous Mesoporous Mater. 32 (1999) 279.
[56] Z. Li, C.G. Xia, X.M. Hang, J. Mol. Catal. A 185 (2002) 47.
[57] J. Luo, S.L. Suib, Chem. Commun. (1997) 1031.
[58] V. Escax, M. Impéror-Clerc, D. Bazin, A. Davidson, C.R. Chim. 8 (2005) 663.
[59] J.S. Choi, D.J. Kim, S.H. Chang, W.S. Ahn, Appl. Catal. A 254 (2003) 225.
[60] A.Y. Khodakov, A. Griboval-Constant, R. Bechara, V.L. Zholobenko, J. Catal. 206 (2002) 230.
[61] R. Craciun, B. Nentwick, K. Hadjiivanov, H. Knözinger, Appl. Catal. A 243 (2003) 67.
[62] M. Grün, K.K. Unger, A. Matsumoto, K. Tsutsumi, in: B. McEnaney, J.T. Mays, J. Rouquerol, F. Rodriguez-Reinoso, K.S.W. Sing, K.K. Unger (Eds.), Characterization of Porous Solids IV, The Royal Society of Chemistry, 1997, p. 81.
[63] S.J. Gregg, K.S.W. Sing, Adsorption, Surface Area and Porosity, Academic Press, London, 1982.
[64] M. Jaroniec, M. Kruk, J.P. Olivier, Langmuir 15 (1999) 5410.
[65] M. Kruk, M. Jaroniec, A. Sayari, J. Phys. Chem. B 101 (1997) 583.
[66] A. Sayari, Y. Yang, J. Phys. Chem. B 104 (2000) 4385.
[67] X. Dong, W. Shen, Y. Zhu, L. Xiong, J. Gu, J. Shi, Microporous Mesoporous Mater. 81 (2005) 235.
[68] X. Sun, C. Ma, L. Zeng, Y. Wang, H. Li, Mater. Res. Bull. 37 (2002) 331.
[69] R.K. Rana, R. Viswanathan, Catal. Lett. 52 (1998) 25.
[70] J. Ryczkowski, J. Goworek, W. Gac, S. Pasieczna, T. Borowiecki, Thermochim. Acta 434 (2005) 2.
[71] Z. Zhang, J. Suo, X. Zhang, S. Li, Appl. Catal. A 179 (1999) 11.
[72] Z. Li, L. Gao, S. Zheng, Mater. Lett. 57 (2003) 4605.
[73] S. Vetrivel, A. Pandurangan, J. Mol. Catal. A 217 (2004) 165.
[74] S. Shylesh, A.P. Singh, J. Catal. 233 (2005) 359.
[75] A.K.H. Nohman, H.M. Ismail, G.A.M. Hussein, J. Anal. Appl. Pyrol. 34 (1995) 265.
[76] D. Dollimore, K.H. Tonge, in: G.W. Schwab (Ed.), Proceedings of the 5th International Symposium on the Reactivity of Solids, Elsevier, Amsterdam, 1965, p. 497.
[77] M.I. Zaki, M.A. Hasan, L. Pasupulety, K. Kumari, Thermochim. Acta 303 (1997) 171.
[78] B.R. Strohmeier, D.M. Hercules, J. Phys. Chem. 88 (1984) 4922.
[79] Y. Liu, M. Luo, Z. Wei, Q. Xin, P. Ying, C. Li, Appl. Catal. B 29 (2001) 61.
[80] S.V. Tsybulya, G.N. Kryukova, T.A. Kriger, P.G. Tsyrul'ni, Kinet. Catal. 44 (2003) 287.
[81] Y. Wang, Z. Song, D. Ma, H. Luo, D. Liang, X. Bao, J. Mol. Catal. A 149 (1999) 51.
[82] W. Weimin, Y. Yongnian, Z. Jiayu, Appl. Catal. A: Gen. 133 (1995) 81.

[83] M. Selvaraj, P.K. Sinha, K. Lee, I. Ahn, A. Pandurangan, T.G. Lee, Microporous Mesoporous Mater. 78 (2005) 139.
[84] M. Kantcheva, M.U. Kucukkal, S. Suzer, J. Mol. Struct. 482 (1999) 19.
[85] Z.-Y. Yuan, H.T. Ma, Q. Luo, W. Zhou, Mater. Chem. Phys. 77 (2002) 299.
[86] N. Novak Tusar, N. Zabukovec Logar, G. Vlaic, I. Arcon, D. Arcon, N. Daneu, V. Kucic, Microporous Mesoporous Mater. 82 (2005) 129.
[87] A. Machocki, T. Ioannides, B. Stasinska, W. Gac, G. Avgouropoulos, D. Delimaris, W. Grzegorczyk, S. Pasieczna, J. Catal. 227 (2004) 282.
[88] G.G. Xia, Y.G. Yin, W.S. Willis, J.Y. Wang, S.L. Suib, J. Catal. 185 (1999) 91.
[89] A. Jentys, N.H. Pham, H. Vinek, M. Englisch, J.A. Lercher, Catal. Today 39 (1998) 311.
[90] S.L. Suib, Curr. Opin. Solid State Mater. Sci. 3 (1998) 63.
[91] N.D. Ivanova, S.V. Ivanov, E.I. Boldyrev, G.V. Sokol'skii, I.S. Makeeva, Russ. J. Appl. Chem. 75 (2002) 1420.
[92] M. Haruta, A. Ueda, S. Tsubota, R.M. Sanchez, Catal. Today 29 (1996) 443.